JGR Atmospheres

RESEARCH ARTICLE
10.1029/2020JD032851

Upward Negative Leaders in Positive Upward Lightning in Winter: Propagation Velocities, Electric Field Change Waveforms, and Triggering Mechanism

Ting Wu[1], **Daohong Wang**[1], **and Nobuyuki Takagi**[1]

[1]Department of Electrical, Electronic and Computer Engineering, Gifu University, Gifu, Japan

Key Points:

- Three-dimensional velocities of 24 UNLs range from 1.8 to 27.9×10^5 m/s with a mean value of 10.4×10^5 m/s
- Radiation field waveforms produced by UNLs are distinctly different from those produced by other types of negative stepped leaders
- UNLs are mainly triggered by nearby (a few km) strong negative strokes combined with following in-cloud positive leaders

Correspondence to:
T. Wu,
tingwu@gifu-u.ac.jp

Citation:
Wu, T., Wang, D., & Takagi, N. (2020). Upward negative leaders in positive upward lightning in winter: Propagation velocities, electric field change waveforms, and triggering mechanism. *Journal of Geophysical Research: Atmospheres*, *125*, e2020JD032851. https://doi.org/10.1029/2020JD032851

Received 31 MAR 2020
Accepted 3 AUG 2020
Accepted article online 6 AUG 2020

Abstract Upward negative leaders (UNLs) in positive upward lightning are rarely observed. In this study, 24 UNLs observed by the Fast Antenna Lightning Mapping Array during winter thunderstorms in Japan are analyzed. Three-dimensional velocities of UNLs are calculated, and it is found that velocities during the upward propagation stage range from 1.8 to 27.9×10^5 m/s with a mean value of 10.4×10^5 m/s, and they are always larger than velocities during the following horizontal propagation stage. UNLs produce distinctive electric field change waveforms with V-shaped overall change trend, with small pulses at the beginning when UNLs start, large pulses during upward propagations, and small pulses again when UNLs turn into horizontal directions. Pulses produced by UNLs are mainly unipolar but sometimes also bipolar. Pulse interval, pulse width, rise time, and fall time are calculated for waveforms produced by five UNLs. Pulse intervals range from 13.7 to 18.9 μs. Pulse width, rise time, and fall time are on average 5.8, 3.3, and 2.4 μs, respectively. All UNLs are preceded by other discharges. Strong negative strokes including some special types of strokes usually precede initiations of UNLs by tens of milliseconds. These negative strokes are usually found only a few kilometers away from UNLs. It is speculated that these negative strokes along with following in-cloud positive leaders contribute to the depletion of negative charges in thunderclouds, which result in positive electric field changes (atmospheric electricity sign convention) large enough for initiations of UNLs.

1. Introduction

Unlike normal lightning flashes which originate inside thunderclouds, upward lightning flashes start with upward leaders from tall grounded objects and pose particular threats to tall buildings, towers, and windmills. Upward lightning flashes are classified into positive and negative ones according to the polarity of charges transferred to the ground. Positive upward flashes start with upward negative leaders (UNLs) and transfer positive charges to the ground, and negative upward flashes start with upward positive leaders (UPLs) and transfer negative charges to the ground. Due to the fact that positive leaders generally require a weaker electric field to initiate (e.g., Williams, 2006), negative upward flashes are much more frequent than positive upward flashes. For example, studies of upward flashes at the Gaisberg Tower show that positive upward flashes only account for about 4% (Watanabe et al., 2019; Zhou et al., 2012a). As a result, compared to upward negative flashes, upward positive flashes are much less well studied.

It has been clear that upward flashes can occur with or without preceding lightning discharges, called "other-triggered" and "self-initiated" upward flashes, respectively (e.g., Wang et al., 2008). Numerous studies have been contributed to the triggering mechanism of upward negative flashes (Guimarães et al., 2014; Jiang et al., 2014; Pineda et al., 2019; Qi et al., 2018; Saba et al., 2016; Sunjerga et al., 2020; Takagi et al., 2006; Wang et al., 2008; Wang & Takagi, 2012a; Warner, 2012; Warner et al., 2012; Warner et al., 2014; Wu, Lyu, et al., 2019; Yuan et al., 2017; Zhou et al., 2012b; Zhu et al., 2019). One interesting phenomenon is that the ratio between other-triggered and self-initiated upward negative flashes varies significantly in different studies (e.g., Saba et al., 2016; Warner et al., 2012; Warner et al., 2014; Zhou et al., 2012b). Apparently, factors contributing to the different ratios at least include seasons, thunderstorm characteristics, and properties of tall objects. For other-triggered upward negative flashes or UPLs, observations show that they can be triggered directly by positive return strokes (Jiang et al., 2014; Wu, Lyu, et al., 2019; Zhou et al., 2012b) or by approaching in-cloud negative leaders (Saba et al., 2016; Yuan et al., 2017). By contrast, triggering mechanisms of upward positive flashes or UNLs are still poorly understood. So far, only a handful of upward positive

flashes or UNLs have been analyzed along with preceding lightning discharges (Heidler et al., 2015; Lu et al., 2009; Wang & Takagi, 2012a, 2012b; Zhou et al., 2012b), and it is still not clear what kind of lightning discharges can trigger UNLs.

Due to the rarity of upward positive flashes, UNLs, the most essential component of upward positive flashes, are also poorly understood. UNLs are apparently negative stepped leaders. Other forms of negative stepped leaders include downward negative stepped leaders in −CG flashes and initial negative leaders during the preliminary breakdown (PB) stage in intracloud (IC) and CG flashes, both of which have been extensively studied using various types of devices, such as high-speed videos (e.g., Hill et al., 2011; Stolzenburg et al., 2013), electric field change (E-change) meters (e.g., Beasley et al., 1982; Krider et al., 1977), interferometers (e.g., Shao et al., 1995; Shao & Krehbiel, 1996), and low-frequency (LF) lightning mapping systems (e.g., Shi et al., 2019a, 2019b; Wu et al., 2015). UNLs are similar to downward stepped leaders in −CG flashes in the respect that both propagate near the ground and largely in the vertical direction. UNLs are also similar to initial leaders in PB stages in the respect that both are the initial leader process in a lightning flash. Therefore, a natural question that arises is what are the differences and similarities between UNLs and the other two types of negative stepped leaders that we are already familiar with.

In this paper, we will analyze 24 UNLs observed in winter in the Hokuriku region of Japan with an LF lightning mapping system called Fast Antenna Lightning Mapping Array (FALMA). Velocities, E-change waveforms, and discharges preceding these UNLs will be analyzed to shed some light on several basic properties of this rare phenomenon.

2. Data

Data were obtained during the winter observation from December 2018 to March 2019 in the Hokuriku region of Japan, which is famous for frequent lightning flashes during the winter season. During the observation, a FALMA system consisting of 14 sites were set up. The FALMA is a three-dimensional (3-D) LF lightning mapping system as described in Wu et al. (2018). Locations of the 14 sites are shown in Figure 1. Each site has a fast antenna working in the frequency band of 500 Hz to 500 kHz. Distances between neighboring sites are from about 10 to 20 km. Triggered E-change signals are recorded with a sampling rate of 10 MS/s. The recording length of each trigger is at least 2 s with the pretrigger length of at least 0.5 s.

A total of 24 UNLs was identified. Initiation locations of these UNLs are shown as red crosses in Figure 1. UNLs were identified based on their 3-D location results and multisite E-change waveforms. Upward leaders initiated from near the ground producing negative pulses (atmospheric electricity sign convention) at all observation sites during their upward propagations are identified as UNLs. Further, their initiation locations are examined in Google Earth to make sure there are tall buildings or towers within several hundred meters or they are in mountains. Information of these UNLs is summarized in Table 1 and will be described in detail in section 3. All UNLs were preceded by other discharges, and only one UNL was followed by a positive return stroke.

3. Results

3.1. Velocities of UNLs

Velocities in 3-D during upward propagation stages (V_u) of all 24 UNLs are estimated. Eighteen UNLs also show horizontal propagations after upward propagations, and 3-D velocities during horizontal propagation stages (V_h) for these 18 UNLs are estimated as well.

Figure 2 shows an example of an UNL in an upward positive flash and illustrates the method to estimate 3-D velocities. Figure 2a shows the height-time view of the whole upward positive flash with preceding discharges. Colored sources indicate the UNL. Figures 2b and 2c show the E-change waveform and height-time view of the UNL. We can see the upward leader produced negative pulses, the same polarity as that produced by positive return strokes, confirming that the leader carried negative charges upward. The 3-D mapping results of the UNL are shown in Figures 2d–2f. The 3-D velocities are estimated using a method similar to that described in section 3.2 in Wu, Wang, and Takagi (2019). Because the leader does

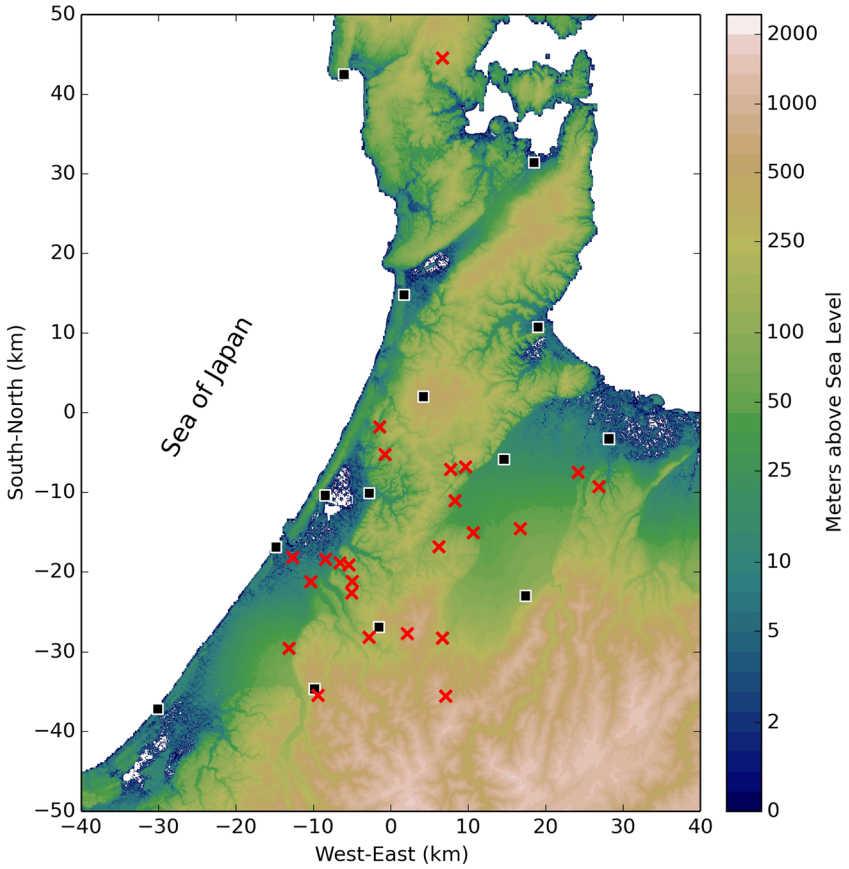

Figure 1. Observation sites of the FALMA (black squares) and initiation locations of upward negative leaders analyzed in this paper (red crosses). The origin (0, 0) corresponds to the latitude and longitude of (36.76°N, 136.76°E).

not propagate in a straight line, several nodes (black diamonds in Figures 2d–2f) are added to divide the leader into roughly straight segments in 3-D. The 3-D distance of each leader source relative to the initiation location is calculated along the straight segments. The 3-D distance versus the time difference between each leader source and the first source are plotted in Figure 2h. Sources before the vertical dashed line are identified as the ones during the upward propagation stage and those after the vertical dashed line are identified as the ones during the horizontal propagation stage. Linear regressions are made for sources in these two stages, and velocities are calculated as the slopes of the regression lines. For the case in Figure 2h, the red dashed line is the regression line for the upward propagation stage, and the velocity V_u is 9.6×10^5 m/s. The blue dashed line is the regression line for the horizontal propagation stage, and the velocity V_h is 4.5×10^5 m/s.

With this method, velocities of V_u are calculated for all 24 UNLs, and velocities of V_h are calculated for 18 UNLs showing horizontal propagations. The results are listed in Table 1, and the distributions are shown in Figures 3a and 3b. Values of V_u range from 1.8 to 27.9×10^5 m/s, the maximum being about 1 order of magnitude larger than the minimum. It is interesting to note that velocities of UPLs from tall objects or in triggered lightning have even larger variations, with the maximum on the order of 10^6 m/s (Yoshida et al., 2010) while the minimum on the order of 10^4 m/s (Edens et al., 2012). The mean value of V_u is 10.4×10^5 m/s and the median value is 9.6×10^5 m/s for 24 UNLs in this study. Most results are smaller than 16×10^5 m/s. Velocities of UNLs in this study are generally larger than the few cases reported outside of Japan (Heidler et al., 2015; Pu et al., 2017; Qiu et al., 2019) but are in general agreement with observations in winter thunderstorms in Japan (Huang et al., 2018; Miki et al., 2014). It should be noted that these previous estimations of UNL velocities were all based on high-speed video observations, so the results were all 2-D estimations and were only for the initial portion of UNLs.

Table 1
Information of 24 UNLs Analyzed in This Paper

Event	Date and time	V_u ($\times 10^5$ m/s)	V_h ($\times 10^5$ m/s)	Horizontal propagation altitude (km)	Horizontal propagation temperature (°C)	Preceding discharges
1	17/12/2018 13:50:40	9.0	—	—	—	IC (negative leader propagating away)
2	17/12/2018 19:03:56	7.3	—	—	—	Special negative stroke ($\Delta d = 1.0$ km, $\Delta t = 50.0$ ms)
3	17/12/2018 20:47:04	4.9	2.2	4.8	−28.4	−RS (short predischarge) ($\Delta d = 0.8$ km, $\Delta t = 19.9$ ms)
4	17/12/2018 20:51:54	9.6	4.5	4.5	−25.9	Special negative stroke ($\Delta d = 0.7$ km, $\Delta t = 58.8$ ms)
5	17/12/2018 20:54:01	9.9	1.6	4.0	−23.1	−RS (short predischarges) ($\Delta d = 2.0$ km, $\Delta t = 22.9$ ms)
6	18/12/2018 14:51:40	9.6	5.7	3.0	−16.4	IC
7	18/12/2018 23:48:02	27.9	5.9	3.9	−21.8	−RS (short predischarges) ($\Delta d = 2.7$ km, $\Delta t = 53.7$ ms)
8	18/12/2018 23:49:40	14.5	5.8	4.1	−23.1	−RS (short predischarges) ($\Delta d = 3.1$ km, $\Delta t = 43.0$ ms)
9	19/12/2018 08:47:04	6.9	2.5	4.1	−21.6	−RS (short predischarges) ($\Delta d = 2.4$ km, $\Delta t = 13.3$ ms)
10	19/12/2018 13:38:05	10.9	0.9	3.7	−18.6	IC (−RS 500 ms ago) (negative leader propagating away)
11	19/12/2018 13:41:36	20.5	2.8	2.8	−11.3	−RS ($\Delta d = 5.9$ km, $\Delta t = 148.3$ ms)
12	19/12/2018 17:50:44	9.2	7.3	1.6	−4.5	IC
13	19/12/2018 18:03:22	2.6	—	—	—	−RS ($\Delta d = 1.7$ km, $\Delta t = 23.3$ ms)
14	19/12/2018 18:06:24	15.3	2.0	3.7	−18.6	Special negative stroke ($\Delta d = 0.8$ km, $\Delta t = 68.6$ ms)
15	17/1/2019 17:19:09	14.4	—	—	—	+RS (downward negative leader before) ($\Delta d = 11.0$ km, $\Delta t = 93.4$ ms)
16	17/1/2019 20:26:14	3.6	1.8	3.3	−19.1	−RS (short predischarges) ($\Delta d = 2.6$ km, $\Delta t = 90.6$ ms)
17	20/1/2019 14:54:12	11.6	3.9	3.1	−10.7	+RS (IC discharges after) ($\Delta d = 22.1$ km, $\Delta t = 243.8$ ms)
18	25/1/2019 20:46:08	14.8	4.7	2.3	−12.3	LBE-like pulse ($\Delta d = 1.5$ km, $\Delta t = 15.5$ ms)
19	25/1/2019 20:46:34	4.3	1.9	2.8	−15.8	LBE-like pulse ($\Delta d = 0.7$ km, $\Delta t = 49.2$ ms)
20	25/1/2019 22:51:37	7.5	—	—	—	LBE-like pulse ($\Delta d = 4.3$ km, $\Delta t = 8.9$ ms)
21	25/1/2019 22:54:03	10.5	6.6	2.6	−14.5	LBE-like pulse ($\Delta d = 14.4$ km, $\Delta t = 397.9$ ms)
22	28/1/2019 18:05:36	1.8	—	—	—	−RS (short predischarges) ($\Delta d = 3.2$ km, $\Delta t = 30.8$ ms)
23	28/1/2019 18:16:09	9.1	4.7	3.7	−23.7	LBE-like pulse ($\Delta d = 0.8$ km, $\Delta t = 109.9$ ms)
24	28/1/2019 18:20:55	14.2	4.2	3.5	−22.9	LBE-like pulse ($\Delta d = 2.0$ km, $\Delta t = 60.6$ ms)

Note. V_u = velocity during the upward propagation stage; V_h = velocity during the horizontal propagation stage.

Values of V_h also have a large range, from 0.9 to 7.3×10^5 m/s with a mean value of 3.8×10^5 m/s and a median value of 4.1×10^5 m/s. For all the 18 UNLs showing horizontal propagations, V_u is larger than V_h (Table 1).

The horizontal propagation altitudes and corresponding ambient air temperatures are also analyzed. For each UNL, its horizontal propagation altitude is calculated as the median value of all source altitudes during the horizontal propagation, and the corresponding temperature is calculated based on the radiosonde observation by the Japan Meteorological Agency. The radiosonde observation site was about 80 km away from the center of our observation network, and the data at 9:00 and 21:00 local time were available. The distributions

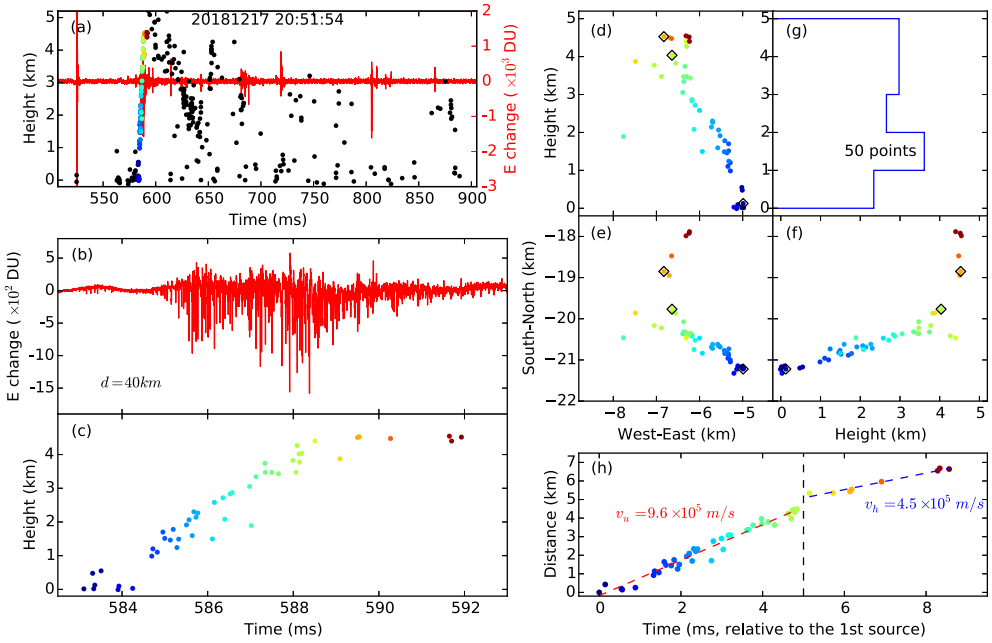

Figure 2. An example of an upward positive lightning flash. (a) Height-time view and E-change waveform of the upward positive lightning flash with preceding discharges. Colored sources correspond to the UNL. (b) E-change waveform and (c) height-time view of the UNL. The value of d indicates the distance between the site recording the waveform and the UNL. (d) Height-distance (from west to east) view, (e) plan view, and (f) distance (from south to north)-height view of the UNL. Black diamonds represent nodes to divide the leader channel into several straight segments. (g) Source distribution along the height. (h) Distance versus time difference of UNL sources relative to the first source. The value of v_u represents the 3-D velocity during the upward propagation (slope of the red dashed line), and the value of v_h represents the 3-D velocity during the horizontal propagation (slope of the blue dashed line).

of propagation altitudes and ambient temperatures are shown in Figures 3c and 3d. Because negative leaders normally propagate horizontally in the positive charge region, these distributions can be treated as distributions for the positive charge region. From Figure 3d, we can see ambient temperatures are mainly from −10°C to −25°C. With such a temperature range for the positive charge region, the negative charge region likely resides below the positive charge region, at the temperature level of about −10°C. Such a normal dipolar charge structure seems to be common for winter thunderstorms in Hokuriku region (Brook et al., 1982).

Values of V_h are found to be correlated with the horizontal propagation altitudes as shown in Figure 3e. Values of V_h show a decreasing trend with increasing altitudes with a correlation coefficient of −0.41. Similar correlation was also observed for initial negative leaders during the PB stage (Wu et al., 2015; Zheng, Shi, et al., 2019) and positive leaders in IC flashes (Wu, Wang, & Takagi, 2019), indicating that there may be a universal relationship between leader velocities and altitudes.

3.2. E-Change Waveform

E-change waveforms of UNLs have been reported before but were mostly measured at close distances (Azadifar et al., 2018; Heidler et al., 2015; Wang & Takagi, 2012b). In fact, the majority of studies on UNLs so far is based on current measurements and/or high-speed video observations on some specific tall objects; remote observations of UNLs are very rare. In this section, we will analyze E-change waveforms of UNLs recorded at tens of kilometers away. This analysis will provide some useful information on the possibility of remotely identifying UNLs. The results can also be used for the comparison with similar leader processes such as PB and stepped leaders, whose E-change waveforms have been extensively measured for decades (e.g., Beasley et al., 1982; Krider et al., 1977).

Figure 4 shows four examples of UNLs with E-change waveforms. Another example can be found in Figure 2. From these examples, we can see that E-change waveforms produced by UNLs have the same

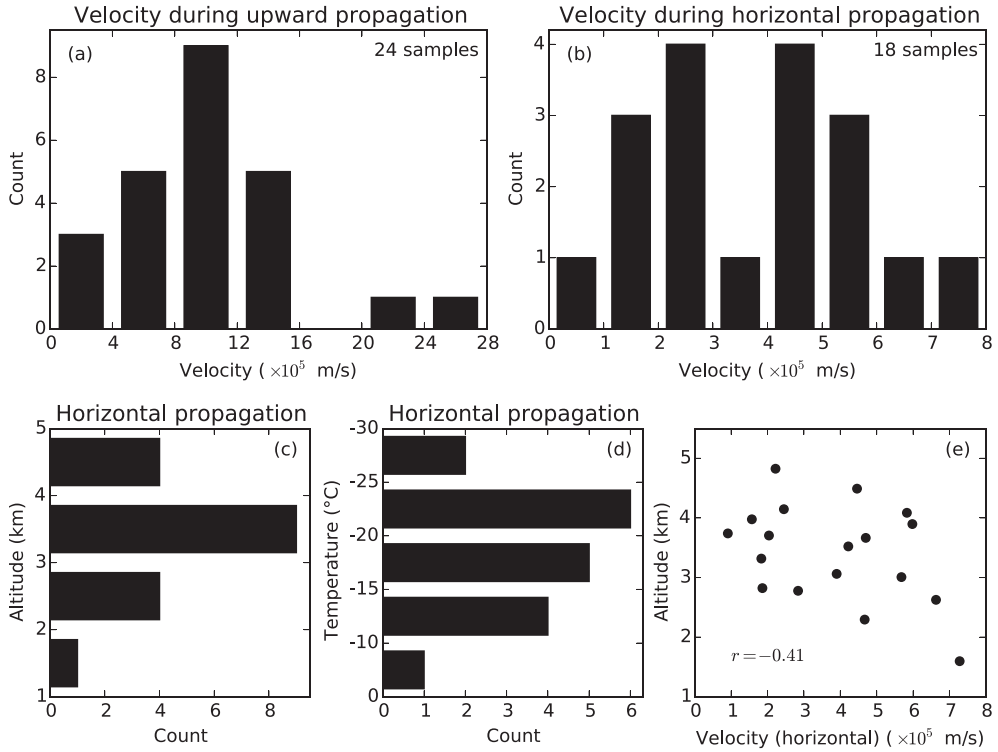

Figure 3. Velocity distributions during the (a) upward and (b) horizontal propagation stages. Distributions of (c) the altitude and (d) the corresponding ambient air temperature of leader horizontal propagations. (e) Altitude versus velocity during the horizontal propagation stage. The value of *r* represents the correlation coefficient.

overall shape, with small pulses at the beginning when UNLs start, large pulses during upward propagations of UNLs, and small pulses again when UNLs turn to horizontal directions. This V-shaped overall change trend is distinctly different from that produced by initial negative leaders in PB stage or negative stepped leaders in −CG flashes.

Figure 5 further shows waveforms on 1-ms time scale produced by these UNLs during their upward propagations. Figures 5a–5d correspond to Figures 4a–4d, and Figure 5e corresponds to Figure 2b. For each UNL, waveforms recorded by two sites with different distances are shown. One site has a distance of 40 to 50 km and the other 10 to 25 km. It is clear that waveforms recorded at these two distances are generally the same.

From Figure 5, we can see that UNLs mainly produce unipolar pulses like negative stepped leaders, but there are also some bipolar pulses. For some pulses, it is difficult to determine whether they are unipolar or bipolar. Pulses seem to be produced continuously, and in many occasions, multiple pulses seem to overlap with each other. Because it is very difficult to set an appropriate criterion to automatically identify all pulses, we manually select pulses for the five examples in Figure 5. The selections are somewhat subjective, and it is indeed difficult to determine what kind of variations should be classified as "pulses." Therefore, all selected pulses are indicated as red and blue crosses in Figure 5, and readers can determine by themselves if too many or too few pulses are selected. The number of selected pulses is indicated by the value of N_p in Figure 5. Numbers of pulses range from 53 to 73, corresponding to average pulse intervals of 13.7 to 18.9 μs. This result is in general agreement with an observation by Huang et al. (2018), who reported that step intervals of four branches in an UNL ranged from 6.6 to 42.9 μs with an average of 19.3 μs.

If we assume that these pulses are produced by stepping processes of UNLs, we can estimate the average step length (l) from the leader velocity (V_u) and the pulse frequency (ρ) with the following equation.

$$l = V_u/\rho \tag{1}$$

where $\rho = N_p/10^{-3}(\mathrm{s}^{-1})$.

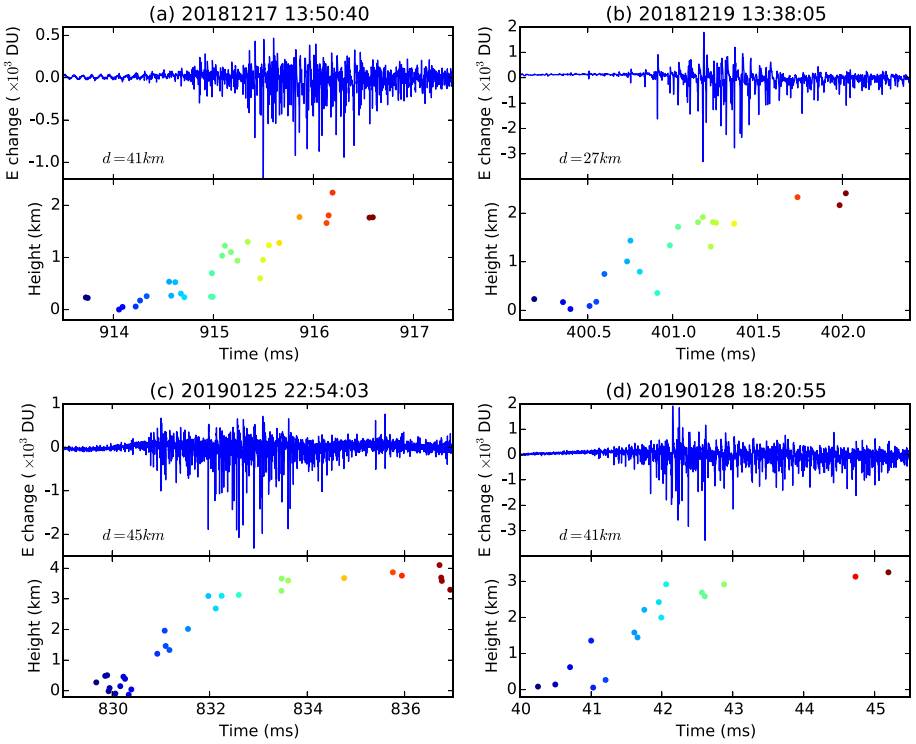

Figure 4. Example of UNLs with E-change waveforms. In each subplot, the upper part shows the E-change waveform, and the lower part shows the height-time view of location results. The value of *d* represents the distance between the site recording the waveform and the UNL. (a)-(d) show four different UNLs.

The estimated average step lengths of these five cases are 15.5, 20.5, 18.0, 25.3, and 13.1 m. These values are somewhat larger than the two UNLs observed by high-speed video cameras (Pu et al., 2017; Qiu et al., 2019). One reason may be that some pulses with small amplitude could not be identified, resulting in an underestimated ρ. Another possible reason is that these two studies only observed the initial ~100 m of the UNLs while our calculations correspond to the stage when UNLs already propagated upward for 1 or 2 km, and it is possible that the step length increases as an UNL propagates upward. Interestingly, three UNLs in winter thunderstorms analyzed by Miki et al. (2014) had average step lengths ranging from 51 to 71 m during propagations in the initial ~500 m.

Pulse rise time, fall time, pulse width, and pulse width at half maximum are also statistically analyzed. Because many pulses overlap with each other, it is difficult to get an accurate result for pulse characteristics. Here we manually select some relatively large pulses without overlapping pulses and calculate the parameters. These selected pulses are indicated by blue crosses in Figure 5. The second selected pulse in Figure 5c is shown in Figure 6a to illustrate definitions of pulse parameters. As many pulses are unipolar pulses, we define rise time as the time from 10% peak to the peak and fall time as the time from the peak to 10% peak as illustrated in Figure 6a, and pulse width is defined as the sum of rise time and fall time. Figures 6b–6d show distributions of rise time, fall time, pulse width, and pulse width at half maximum. We can see the pulse width is mainly from 2 to 8 μs, with the rise time slightly larger than the fall time. The mean values of pulse width, pulse width at half maximum, rise time, and fall time are 5.8, 2.7, 3.3, and 2.4 μs, respectively.

3.3. Triggering Mechanisms

All 24 UNLs are preceded by other discharges, that is, they occur as the initial stage of "other-triggered" upward positive lightning flashes. Information of preceding discharges is summarized in Table 1. It seems most UNLs are preceded by negative strokes, contrary to UPLs, which are usually preceded by positive strokes (e.g., Warner et al., 2012; Zhou et al., 2012b).

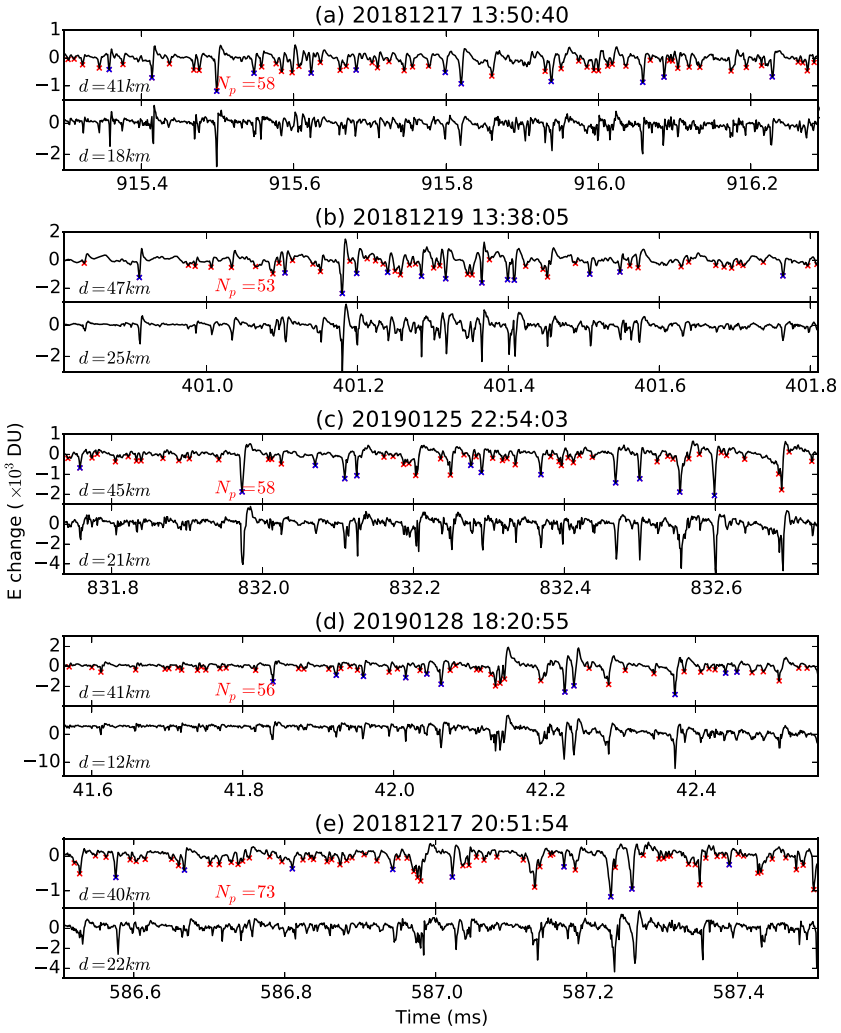

Figure 5. E-change waveforms of UNLs in Figures 4 and 2 in 1-ms time scale. Waveforms recorded by two sites with different distances (represented by the value of d) are shown for each event. The value of N_p represents the number of selected pulses (red and blue crosses). Pulses with blue crosses are further analyzed for pulse parameters shown in Figure 6. (a)-(e) show waveforms in five different UNLs.

The first type of triggering event is called "special negative stroke" (Events 2, 4, and 14 in Table 1). Two examples are shown in Figures 7a and 7b. In each case, we can see a large pulse with positive initial polarity (the same as negative return stroke) occurred about 50 ms before the UNL. The pulse was so large that in every case, it saturated all of our observation sites. The polarity of the pulse indicates that it is produced by a negative stroke, but the stroke may be different from normal negative return strokes because the waveforms show similar rise time and fall time. It is also different from return strokes in that there are only a few pulses lasting for ~200 μs before the main pulse, and no typical PB pulses can be identified. This special type of event has recently been reported by Wada et al. (2020) to be associated with downward terrestrial gamma ray flashes. Two events reported by Wada et al. (2020) had estimated peak currents of −260 and −197 kA. Although we cannot estimate currents of the events we observed, the fact that these events saturated all of the observation sites indicates that they also carried extremely large current. Note that Wada et al. (2020) interpreted this special type of discharge as negative polarity "energetic in-cloud pulse" (Lyu et al., 2015), but according to our recent analysis, it is more likely a type of return stroke occurring in certain special conditions, which is why we call it "special negative stroke" in this study. Detailed analysis will be reported in a follow-up paper.

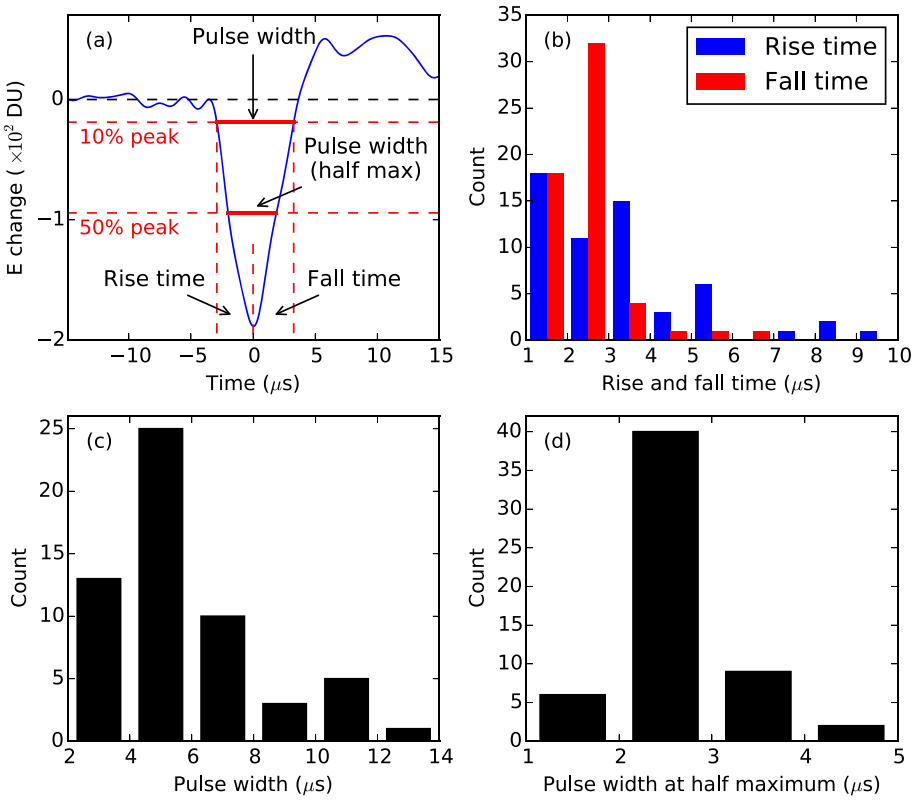

Figure 6. (a) Definitions of pulse parameters. Distributions of (b) rise time and fall time, (c) pulse width, and (d) pulse width at half maximum for those pulses marked by blue crosses in Figure 5.

The second type of triggering event is negative return strokes (Events 3, 5, 7, 8, 9, 11, 13, 16, and 22). It is interesting to note that most of these return strokes have extremely short time differences from the beginning of flashes (denoted as "short predischarges" in Table 1). Two examples are given in Figures 7c and 7d. Discharges before the return strokes in Figures 7c and 7d lasted for only about 300 and 800 μs, respectively. Negative return strokes with such short predischarges were not observed in summer. Even assuming the initiation altitudes of these −CG flashes were only 1 km, we would get the overall velocities of stepped leaders on the order of 10^6 m/s. The high velocity of stepped leaders is usually associated with the large peak current of return strokes (Shi et al., 2019a), indicating that negative return strokes triggering UNLs usually have high peak currents.

The third type of triggering event is bipolar pulses similar to the so-called "large bipolar event" (LBE) reported by Wu et al. (2014) (Events 18, 19, 20, 21, 23 and 24). As analyzed by Wu et al. (2014), LBEs always have the same polarity as negative return strokes and are on average stronger than return strokes. In two of the events (Events 20 and 21), another large pulse occurred before the LBE-like pulse, and these two examples are shown in Figures 7e and 7f. In each example, we can see at least two large pulses before the start of the UNL. The second pulse is similar to the LBE, while the first pulse has an initial small negative change, and it is not clear what kind of discharges produced this pulse. For the case in Figure 7f, discharges before the UNL are not so strong and have a long time different (~400 ms) from the UNL, so it is also possible that the UNL was not associated with the pulses at the beginning.

The fourth type of triggering event is IC discharges (Events 1, 6, 10, and 12). In two of the cases, leader channels are well imaged and are shown in Figure 8. Although some sources were very close to the ground in Figure 8, we confirmed from E-change waveforms that there were no return strokes before the initiation of UNLs. Initiation locations of UNLs are indicated by red diamonds. We can see in each example, leaders passed by the initiation locations with a distance of about 3–4 km and propagated away. About 50 ms after the leaders stopped propagating, UNLs were initiated. It has been reported that approaching negative

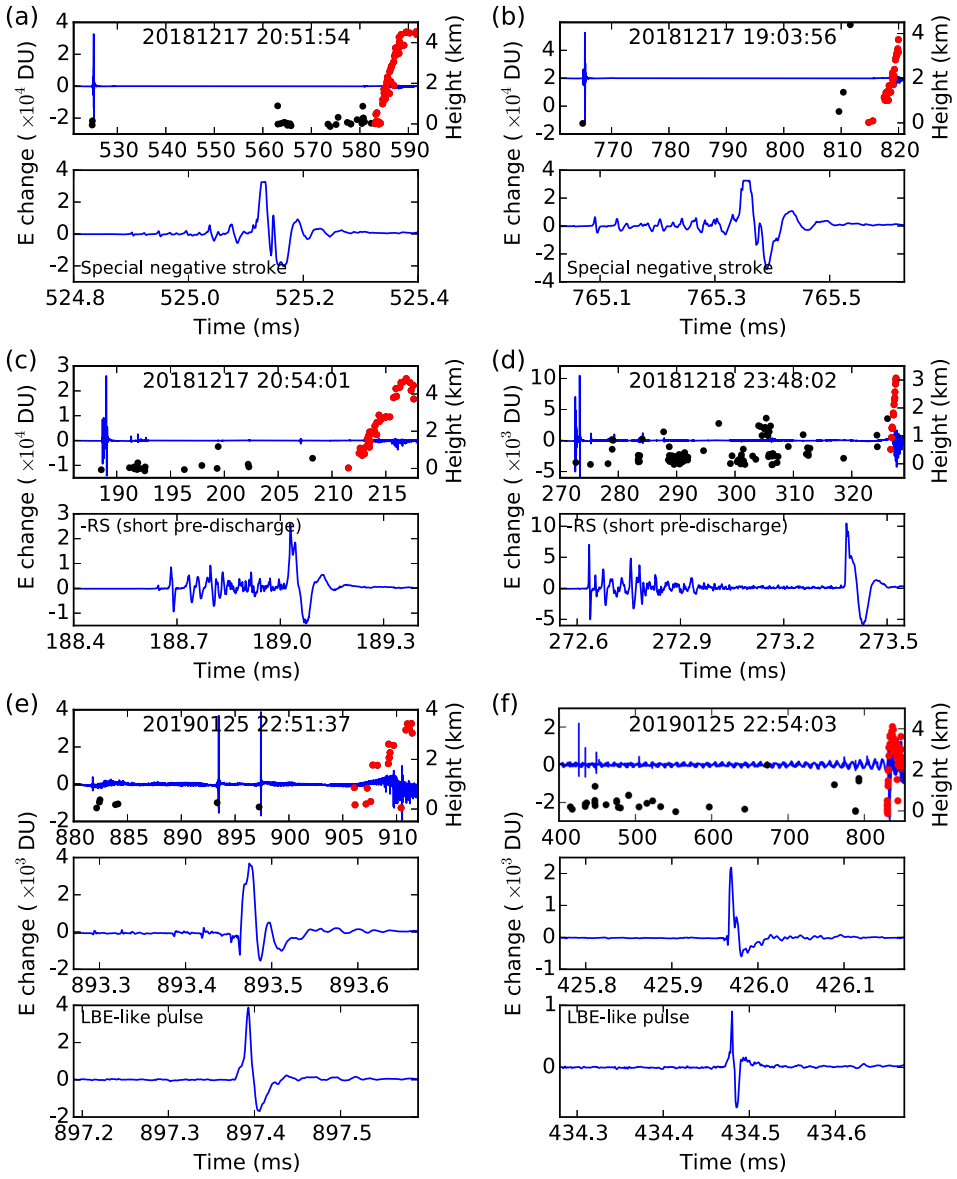

Figure 7. Lightning discharges preceding UNLs. (a and b) Special negative strokes. (c and d) Negative return strokes with extremely short predischarges. (e and f) At least two large pulses including one special pulse with initial small negative change and one LBE-like pulse. In each subplot, the first figure shows E-change waveform and height-time view of location results from the beginning of discharges preceding the UNL to the UNL. Red points represent sources of UNLs. Figures below show expanded views of large pulses before UNLs.

leaders can trigger UPLs (Saba et al., 2016; Yuan et al., 2017), consistent with our observation that negative leaders propagating away preceded initiations of UNLs.

In the remaining two cases (Events 15 and 17), positive return strokes were observed before UNLs. However, it is unlikely that the positive return strokes triggered UNLs. In Event 15, a downward negative leader was observed right before the positive return stroke, and in Event 17, IC discharges were observed after the positive return stroke. It is possible that some in-cloud discharges triggered these UNLs. Triggering mechanisms will be further discussed in section 4.3.

In the case of upward negative lightning, there have been reports that one positive return stroke triggered several UPLs (Warner, 2012; Wu, Lyu, et al., 2019). In this study, although we did not observe multiple UNLs triggered together, it seems not rare that some scattered sources are located near the ground right

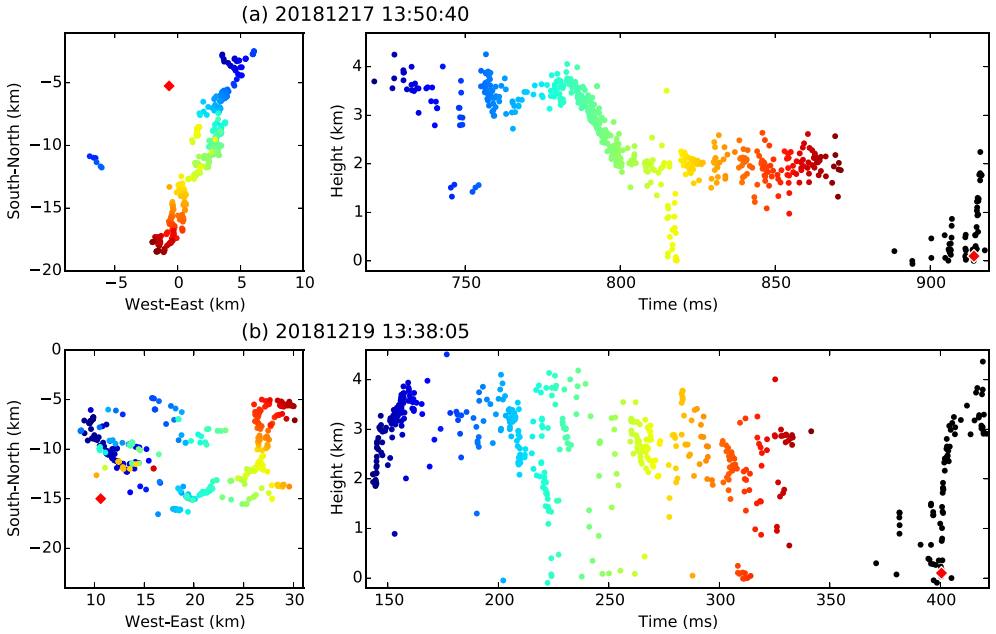

Figure 8. Two examples of UNLs preceded by IC discharges. The left part shows the plan view, and the right part shows the height-time view. Colored points represent sources of IC discharges. Red diamonds represent initiation locations of UNLs. (a) and (b) show two different flashes.

before the onset of UNLs. One example is shown in Figure 9. The UNL started at the time of about 583 ms, and sources of discharges right before along with E-change waveform are shown in Figure 9. In Figure 9a, the blue cross indicates the location of the triggering event (also shown in Figure 7a), the red diamond indicates the initiation location of the UNL, and black triangles indicate locations of transmission towers identified from Google Earth. Interestingly, sources right before the UNL seem to be distributed near transmission towers, and their source altitudes are all lower than 1 km. It seems very likely that these sources are produced by discharges on transmission towers triggered by the same stroke, but these discharges failed to develop into long negative leaders. They may be aborted UNLs as reported by Wang et al. (2008). They can also be corona discharges. Wu et al. (2017) reported that increased sources of corona discharges from tall objects were detected following nearby lightning discharges.

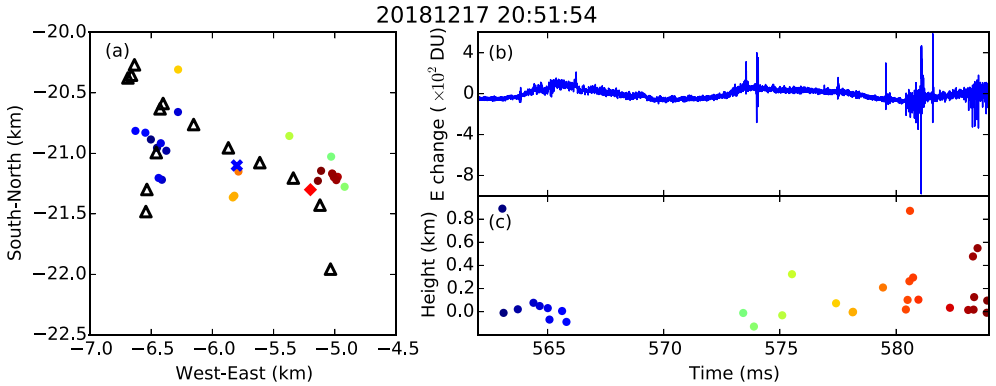

Figure 9. Discharges right before the onset of an UNL. (a) Plan view. The blue cross represents the negative stroke before the UNL (also shown in Figure 7a). The red diamond represents the initiation location of the UNL. Black triangles represent transmission towers. (b) E-change waveform. (c) Height-time view.

4. Discussion

4.1. Comparison of UNLs With Initial Negative Leaders in PB Stage

Both UNLs and initial negative leaders in PB stages of IC and CG flashes serve as the initial leader processes in lightning flashes. However, there are several apparent differences between these two types of leaders.

First, they produce distinctly different E-change waveforms. As shown in Figure 5, pulses produced by UNLs are mainly unipolar pulses. As for pulses produced by initial negative leaders, that is, PB pulses, although they also include narrow unipolar pulses, bipolar pulses with pulse widths of tens of microseconds, called "classic PB pulses," are the primary feature of PB pulses (Marshall et al., 2014; Nag et al., 2009). According to Figure 6, pulse widths of UNL pulses are mostly smaller than 8 μs with a maximum of 13.0 μs. In other words, no classic PB pulses can be found in pulses produced by UNLs. Pulse intervals of UNL pulses are also much shorter than those of PB pulses. For example, pulse intervals of PB pulses had a mean value of 73 μs reported by Nag and Rakov (2008) and 152 μs reported by Baharudin et al. (2012). By contrast, E-change waveforms of the five UNLs in Figure 5 had average pulse intervals smaller than 20 μs.

High-speed video observations of initial negative leaders in PB stages have established that each step of the initial leader corresponds to a classic PB pulse (Campos & Saba, 2013; Stolzenburg et al., 2013, 2014; Wilkes et al., 2016). For UNL pulses, however, it seems that all the narrow and small pulses are produced by leader steps according to the analysis in section 3.2.

Step lengths of UNLs seem to be much shorter than those of initial negative leaders. Leader steps in the PB stage of a −CG flash reported by Stolzenburg et al. (2014) had step lengths ranging from 30 to 183 m with a mean value of 89 m. Step lengths of initial leaders in hundreds of IC flashes estimated by Wu et al. (2015) ranged from 20 to 426 m with a mean value of 113 m. By contrast, step lengths of five UNLs estimated in this study range from 13.1 to 25.3 m, and step lengths of two UNLs observed by high speed videos reported by Pu et al. (2017) and Qiu et al. (2019) were smaller than 10 m.

Velocities of UNLs analyzed in this study have large variations, from 1.8 to 27.9×10^5 m/s. Velocities of initial negative leaders in both −CG and IC flashes also have large variations. Shi et al. (2019a) reported that vertical velocities of initial negative leaders in 279 −CG flashes ranged from 1.6 to 12.4×10^5 m/s. Wu et al. (2015) reported that vertical velocities of initial negative leaders in 662 IC flashes ranged from 0.5 to 17.8×10^5 m/s. Initial leader velocities larger than 10^6 m/s were also reported by Heavner et al. (2002). Based on these results, it seems velocities of UNLs are generally similar to those of initial negative leaders.

Differences between UNLs and initial negative leaders can be partly explained by their different altitudes of occurrences. As demonstrated by Wu et al. (2015), with decreasing initiation altitudes, initial negative leaders in IC flashes produce more frequent pulses and have shorter step lengths. If this altitude-related correlation can be applied to UNLs, which occur near the ground, small pulse intervals and short step lengths are expected results.

4.2. Comparison of UNLs With Stepped Leaders in −CG Flashes

Both UNLs and stepped leaders in −CG flashes propagate near the ground, and it seems that they have more similarities than differences. First, it seems that they have similar step lengths. Step lengths of stepped leaders in −CG flashes generally range from several meters to a few tens of meters (e.g., Chen et al., 1999; Hill et al., 2011; Qi et al., 2016), consistent with our estimations and previous observations (Miki et al., 2014; Pu et al., 2017; Qiu et al., 2019). Second, although velocities of stepped leaders in −CG flashes are thought to have a typical value of 2×10^5 m/s, they have significant variations in different studies. For example, according to the review by Rakov and Uman (2003, p. 123), velocities of stepped leaders range from 0.3 to 39×10^5 m/s, in general agreement with velocities of UNLs.

One apparent difference between UNLs and stepped leaders in −CG flashes is their E-change waveforms. As shown in Figure 4, E-change waveforms produced by UNLs are very small at the beginning of the leader, and then the amplitude increases until the leader turns into a horizontal direction. Such V-shaped overall change trend was not observed in E-change waveforms produced by stepped leaders in −CG flash. This difference may lie in the fact that formations of UNLs include an initiation process while stepped leaders in −CG flashes do not. Stepped leaders, when they are observed, already have a self-propagating hot channel, which may result in similar peak currents in different steps. On the other hand, for UNLs, no leader channels exist

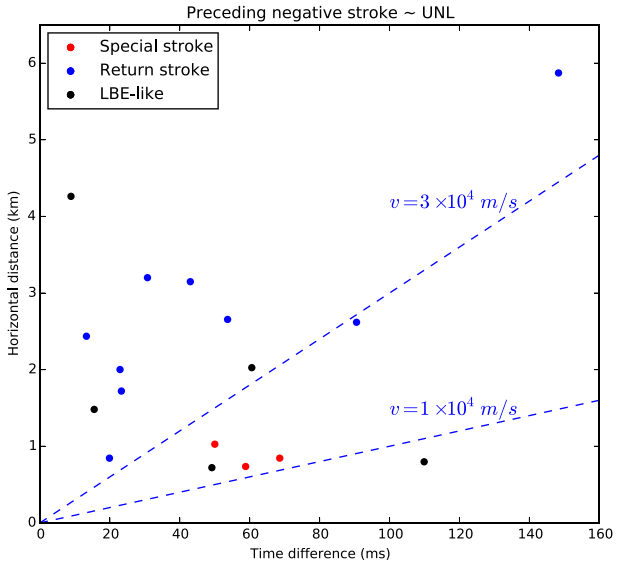

Figure 10. Scatterplot of horizontal distance and time difference between initiation locations of UNLs and preceding negative strokes. Slopes of two blue dashed lines represent two velocity values indicated above.

at the time of their initiations. The formation of leader channels likely consists of different types of processes that have different currents, resulting in obvious variations of E-change pulses.

4.3. Triggering Mechanism of UNLs

Opposite to UPLs, which are usually preceded by positive return strokes (e.g., Warner et al., 2012; Zhou et al., 2012b), UNLs reported in this paper are usually preceded by negative strokes, including "special negative strokes," negative return strokes, and LBE-like pulses as listed in Table 1. All of these strokes produce positive E-changes (atmospheric electricity sign convention), which are necessary for the initiation of UNLs.

However, time differences between these strokes and initiations of UNLs are generally tens of milliseconds, implying that these strokes did not directly trigger UNLs. As for the triggering of UPLs, some UPLs are reported to be preceded by positive return strokes within 1 ms (Jiang et al., 2014; Wu, Lyu, et al., 2019; Zhou et al., 2012b), indicating that these UPLs were likely triggered directly by the preceding positive return strokes. However, many more UPLs were preceded by positive return strokes for a much longer time. For example, according to Figure 6 in Saba et al. (2016), many UPLs were preceded by triggering events for more than 50 ms. Therefore, a more common triggering component for UPLs seems to be approaching negative leaders, which can also create negative E-changes necessary for the initiation of UPLs. This has been confirmed by high-speed video observations (Saba et al., 2016; Yuan et al., 2017). In fact, if we look at the left half of Figure 6 in Saba et al. (2016) and draw a regression line, the slope (corresponding to the ratio between distance and time difference from the triggering event) would be close to 2×10^5 m/s, typical for the velocity of negative leaders propagating in virgin air. This result supports the theory that negative leaders in +CG flashes propagating toward the tall object are responsible for the triggering of UPLs.

Accordingly, we examine a similar mechanism that approaching positive leaders trigger UNLs. Positive leaders are basically invisible to LF systems, so we do not have direct evidence. However, there seem to be some difficulties for this mechanism. First, distances and time differences between triggering events and UNLs do not show any correlation. Figure 10 shows a scatterplot of distances versus time differences for UNLs preceded by negative strokes, and apparently, there is no correlation between these two parameters. We also analyzed distances and time differences between the initiation of preceding flashes and UNLs, and they did not show any correlation either. Second, according to Wu, Wang, and Takagi (2019), positive leaders in −CG and IC flashes propagate with a stable velocity of 1 to 3×10^4 m/s. Two dashed lines representing these two velocities are also plotted in Figure 10, and we can see for many UNLs, distances between preceding strokes and UNLs are too large for positive leaders to traverse within the time differences. For example, Event 9 in Table 1 is preceded by a negative return stroke with a distance of 2.4 km and a time difference of 13.3 ms. A positive leader needs to have a velocity of at least 1.8×10^5 m/s to travel to the tall object before the initiation of the UNL, which is apparently too fast according to the result of Wu, Wang, and Takagi (2019).

One possible explanation for these discrepancies is that positive leaders do not have to propagate to a location right above a tall object to trigger UNLs. Triggering events listed in Table 1 are generally less than 3 km away from UNLs, close enough to have significant influences on electric fields at initiation locations of UNLs. The relatively large time differences between triggering events and UNLs may be due to the fact that UNLs are relatively difficult to be initiated, and a negative stroke alone is usually not able to produce E-changes large enough for the initiation of UNLs. After the negative stroke, in-cloud positive leaders, although being a few kilometers away from the tall object, keep draining negative charges in thunderclouds and contribute to further increases of positive E-changes at the tall object until the initiation of UNLs.

Further, we speculate that unlike the triggering of UPLs, which favorites an approaching negative leader, the triggering of UNLs does not require an approaching positive leader but a nearby positive leader due to the fact that positive leaders travel much more slowly than negative leaders. Assuming a positive leader velocity of 2×10^4 m/s, the leader only moves for 2 km in 100 ms, so even if it moves away from a tall object, it still has significant influences on E-changes on the tall object after 100 ms, as long as the leader starts at a location close enough to the tall object. Therefore, it is likely that the direction of positive leaders, whether approaching or not, is not important. The more essential factor for the triggering of UNLs is that the triggering flash starts close to the tall object from which UNLs are to be triggered. This is why in our study, distances between triggering events and UNLs are generally only a few kilometers, much smaller than those for UPLs (mostly from 10 to 40 km as reported by Saba et al., 2016), while time differences are normally tens of milliseconds, comparable to those for UPLs.

Apart from those UNLs preceded by negative strokes, as analyzed in section 3.3, four UNLs were preceded by IC discharges, and in two of them, negative leaders propagating away from the initiation locations were observed. Negative leaders propagating away can also produce positive E-changes which are necessary for the initiation of UNLs. There are also two UNLs preceded by positive return strokes. However, it is unlikely that positive return strokes can trigger UNLs; some not-well-resolved leader processes may be the triggering component.

It is also interesting to note that different types of preceding discharges appear to cluster in certain periods. For example, according to Table 1, all LBE-type discharges occurred in 25 and 28 January. This feature indicates that different types of triggering events are likely associated with different charge structures. Indeed, winter thunderstorms in Japan sometimes have quite complicated charge structures (e.g., Wang et al., 2018; Zheng, Wang, Zhang, Wu, & Takagi, 2019), which may result in the special types of triggering events such as the special negative strokes and LBE-like discharges, and the triggering mechanism of UNLs may well be much more complicated than what we have proposed.

In summary, lightning discharges efficient in triggering UNLs seem to be a strong negative stroke combined with following in-cloud positive leaders. These positive leaders need to be within a few kilometers from tall objects, but they do not have to propagate toward tall objects.

5. Conclusions

With the observation of the FALMA in winter thunderstorms in Japan, 24 UNLs were recorded, and their velocities, E-change waveforms, and triggering mechanism are analyzed. Major findings are summarized as follows.

The 3-D velocity during the upward propagation stage of UNLs ranges from 1.8 to 27.9×10^5 m/s with a mean value of 10.4×10^5 m/s. When an UNL turns into a horizontal direction after the upward propagation stage, the velocity always decreases. Velocities during the horizontal propagation stage range from 0.9 to 7.3×10^5 m/s with a mean value of 3.8×10^5 m/s. Velocities of UNLs seem to be generally similar to velocities of downward stepped leaders in −CG flashes and initial negative leaders in PB stages.

The E-change waveforms of UNLs measured at tens of kilometers show a distinctive V-shaped overall change trend. The waveforms include small pulses at the beginning when UNLs start, large pulses during the upward propagations of UNLs, and small pulses again when UNLs turn into horizontal directions. UNLs produce mainly unipolar pulses but also some bipolar pulses. Pulses produced by five UNLs are statistically analyzed. Pulse intervals range from 13.7 to 18.9 μs. Pulse width, pulse width at half maximum, rise time, and fall time are on average 5.8, 2.7, 3.3, and 2.4 μs, respectively. E-change waveforms of UNLs are distinctly different from those produced by other types of negative leaders, such as downward stepped leaders in −CG flashes and initial negative leaders in PB stages.

Negative strokes are usually found tens of milliseconds before initiations of UNLs. Probably due to special conditions in winter, these negative strokes include some special types of discharges that are different from normal negative return strokes, but they all have the same polarity as negative return strokes. Further analysis indicates that these negative strokes did not directly trigger UNLs; nearby in-cloud positive leaders following these strokes further deplete negative charges in thunderclouds and contribute to further positive

E-changes (atmospheric electricity sign convention) on tall objects, which seems to be essential for initiations of UNLs.

Data Availability Statement

E-change waveform data of UNLs analyzed in this study can be downloaded from the link (http://doi.org/10.5281/zenodo.3733900).

Acknowledgments
This work was supported by the Ministry of Education, Culture, Sports, Science, and Technology of Japan (Grants 16H04315 and 18K13618).

References

Azadifar, M., Rubinstein, M., Rachidi, F., Rakov, V.A., Pavanello, D., & Metz, S. (2018). On the similarity of electric field signatures of upward and downward negative leaders. Paper presented at the 34th International Conference on Lightning Protection (ICLP).

Baharudin, Z. A., Ahmad, N. A., Fernando, M., Cooray, V., & Mäkelä, J. S. (2012). Comparative study on preliminary breakdown pulse trains observed in Johor, Malaysia and Florida, USA. *Atmospheric Research*, *117*(11), 111–121. https://doi.org/10.1016/j.atmosress.2012.01.012

Beasley, W. H., Uman, M. A., & Rustan, P. L. (1982). Electric fields preceding cloud-to-ground lightning flashes. *Journal of Geophysical Research*, *87*(C7), 4883–4902. https://doi.org/10.1029/JC087iC07p04883

Brook, M., Nakano, M., & Krehbiel, P. (1982). The electrical structure of the Hokuriku winter thunderstorm. *Journal of Geophysical Research*, *87*(C2), 1207–1215. https://doi.org/10.1029/JC087iC02p01207

Campos, L. Z., & Saba, M. M. F. (2013). Visible channel development during the initial breakdown of a natural negative cloud-to-ground flash. *Geophysical Research Letters*, *40*(17), 4756–4761. https://doi.org/10.1002/grl.50904

Chen, M., Takagi, N., Watanabe, T., Wang, D., Kawasaki, Z. I., & Liu, X. (1999). Spatial and temporal properties of optical radiation produced by stepped leaders. *Journal of Geophysical Research*, *104*(D22), 27,573–27,584. https://doi.org/10.1029/1999JD900846

Edens, H. E., Eack, K. B., Eastvedt, E. M., Trueblood, J. J., Winn, W. P., Krehbiel, P. R., et al. (2012). VHF lightning mapping observations of a triggered lightning flash. *Geophysical Research Letters*, *39*(19), L19807. https://doi.org/10.1029/2012GL053666

Guimarães, M., Araujo, L., Pereira, C., Mesquita, C., & Visacro, S. (2014). Assessing currents of upward lightning measured in tropical regions. *Atmospheric Research*, *149*, 324–332. https://doi.org/10.1016/j.atmosres.2014.01.005

Heavner, M. J., Smith, D. A., Jacobson, A. R., & Sheldon, R. J. (2002). LF/VLF and VHF lightning fast-stepped leader observations. *Journal of Geophysical Research*, *107*(D24), 4791. https://doi.org/10.1029/2001JD001290

Heidler, F. H., Manhardt, M., & Stimper, K. (2015). Characteristics of upward positive lightning initiated from the Peissenberg Tower, Germany. *IEEE Transactions on Electromagnetic Compatibility*, *57*(1), 102–111. https://doi.org/10.1109/TEMC.2014.2359584

Hill, J. D., Uman, M. A., & Jordan, D. M. (2011). High-speed video observations of a lightning stepped leader. *Journal of Geophysical Research*, *116*(D16), D16117. https://doi.org/10.1029/2011JD015818

Huang, H., Wang, D., Wu, T., & Takagi, N. (2018). Formation features of steps and branches of an upward negative leader. *Journal of Geophysical Research: Atmospheres*, *123*(22), 12,597–12,605. https://doi.org/10.1029/2018JD028979

Jiang, R., Qie, X., Wu, Z., Wang, D., Liu, M., Lu, G., & Liu, D. (2014). Characteristics of upward lightning from a 325-m-tall meteorology tower. *Atmospheric Research*, *149*, 111–119. https://doi.org/10.1016/j.atmosres.2014.06.007

Krider, E. P., Weidman, C. D., & Noggle, R. C. (1977). The electric fields produced by lightning stepped leaders. *Journal of Geophysical Research*, *82*(6), 951–960. https://doi.org/10.1029/JC082i006p00951

Lu, W. T., Wang, D. H., Zhang, Y., & Takagi, N. (2009). Two associated upward lightning flashes that produced opposite polarity electric field changes. *Geophysical Research Letters*, *36*, L05801. https://doi.org/10.1029/2008GL036598

Lyu, F., Cummer, S. A., & McTague, L. (2015). Insights into high peak current in-cloud lightning events during thunderstorms. *Geophysical Research Letters*, *42*(16), 6836–6843. https://doi.org/10.1002/2015gl065047

Marshall, T., Schulz, W., Karunarathna, N., Karunarathne, S., Stolzenburg, M., Vergeiner, C., & Warner, T. (2014). On the percentage of lightning flashes that begin with initial breakdown pulses. *Journal of Geophysical Research: Atmospheres*, *119*(2), 445–460. https://doi.org/10.1002/2013JD020854

Miki, M., Miki, T., Asakawa, A., & Shindo, T. (2014). Characteristics of negative upward stepped leaders in positive upward lightning. Paper presented at XV International Conference on Atmospheric Electricity.

Nag, A., DeCarlo, B. A., & Rakov, V. A. (2009). Analysis of microsecond- and submicrosecond-scale electric field pulses produced by cloud and ground lightning discharges. *Atmospheric Research*, *91*(2–4), 316–325. https://doi.org/10.1016/j.atmosres.2008.01.014

Nag, A., & Rakov, V. A. (2008). Pulse trains that are characteristic of preliminary breakdown in cloud-to-ground lightning but are not followed by return stroke pulses. *Journal of Geophysical Research*, *113*(D1), D01102. https://doi.org/10.1029/2007JD008489

Pineda, N., Figueras i Ventura, J., Romero, D., Mostajabi, A., Azadifar, M., Sunjerga, A., et al. (2019). Meteorological aspects of self-initiated upward lightning at the Säntis tower (Switzerland). *Journal of Geophysical Research: Atmospheres*, *124*(24), 14,162–14,183. https://doi.org/10.1029/2019JD030834

Pu, Y., Jiang, R., Qie, X., Liu, M., Zhang, H., Fan, Y., & Wu, X. (2017). Upward negative leaders in positive triggered lightning: Stepping and branching in the initial stage. *Geophysical Research Letters*, *44*(13), 7029–7035. https://doi.org/10.1002/2017GL074228

Qi, Q., Lu, W. T., Ma, Y., Chen, L. W., Zhang, Y. J., & Rakov, V. A. (2016). High speed video observations of the fine structure of a natural negative stepped leader at close distance. *Atmospheric Research*, *178-179*, 260–267. https://doi.org/10.1016/j.atmosres.2016.03.027

Qi, Q., Lyu, W., Wu, B., Ma, Y., Chen, L., & Liu, H. (2018). Three-dimensional optical observations of an upward lightning triggered by positive cloud-to-ground lightning. *Atmospheric Research*, *214*(46), 275–283. https://doi.org/10.1016/j.atmosres.2018.08.003

Qiu, Z., Yang, Y., Qin, Z., Chen, M., Lyu, F., Guo, H., et al. (2019). Optical and current measurements of lightning attachment to the 356-m-high Shenzhen Meteorological Gradient Tower in southern coastal area of China. *IEEE Access*, *7*, 155,372–155,380. https://doi.org/10.1109/ACCESS.2019.2949127

Rakov, V. A., & Uman, M. A. (2003). *Lightning physics and effects*. Cambridge, UK: Cambridge University Press. https://doi.org/10.1017/CBO9781107340886

Saba, M. M. F., Schumann, C., Warner, T. A., Ferro, M. A. S., de Paiva, A. R., Helsdon, J. Jr., & Orville, R. E. (2016). Upward lightning flashes characteristics from high-speed videos. *Journal of Geophysical Research: Atmospheres*, *121*(14), 8493–8505. https://doi.org/10.1002/2016JD025137

Shao, X., Krehbiel, P., Thomas, R., & Rison, W. (1995). Radio interferometric observations of cloud-to-ground lightning phenomena in Florida. *Journal of Geophysical Research*, *100*(D2), 2749–2783. https://doi.org/10.1029/94JD01943

Shao, X. M., & Krehbiel, P. R. (1996). The spatial and temporal development of intracloud lightning. *Journal of Geophysical Research*, *101*(D21), 26,641–26,668. https://doi.org/10.1029/96JD01803

Shi, D., Wang, D., Wu, T., & Takagi, N. (2019a). Correlation between the first return stroke of negative CG lightning and its preceding discharge processes. *Journal of Geophysical Research: Atmospheres*, *124*, 8501–8510. https://doi.org/10.1029/2019JD030593

Shi, D., Wang, D., Wu, T., & Takagi, N. (2019b). Temporal and spatial characteristics of preliminary breakdown pulses in intracloud lightning flashes. *Journal of Geophysical Research: Atmospheres*, *124*(23), 12,901–12,914. https://doi.org/10.1029/2019JD031130

Stolzenburg, M., Marshall, T. C., Karunarathne, S., Karunarathna, N., & Orville, R. E. (2014). Leader observations during the initial breakdown stage of a lightning flash. *Journal of Geophysical Research: Atmospheres*, *119*(21), 12,198–12,221. https://doi.org/10.1002/2014JD021994

Stolzenburg, M., Marshall, T. C., Karunarathne, S., Karunarathna, N., Vickers, L. E., Warner, T. A., et al. (2013). Luminosity of initial breakdown in lightning. *Journal of Geophysical Research: Atmospheres*, *118*(7), 2918–2937. https://doi.org/10.1002/jgrd.50276

Sunjerga, A., Rubinstein, M., Pineda, N., Mostajabi, A., Azadifar, M., Romero, D., et al. (2020). LMA observations of upward lightning flashes at the Säntis Tower initiated by nearby lightning activity. *Electric Power Systems Research*, *181*, 106067. https://doi.org/10.1016/j.epsr.2019.106067

Takagi, N., Wang, D., & Watanabe, T. (2006). A study of upward positive leaders based on simultaneous observation of E-felds and high-speed images. *IEEJ Transactions on Fundamentals and Materials*, *126*(4), 256–259. https://doi.org/10.1541/ieejfms.126.256

Wada, Y., Enoto, T., Nakamura, Y., Morimoto, T., Sato, M., Ushio, T., et al. (2020). High peak-current lightning discharges associated with downward terrestrial gamma-ray flashes. *Journal of Geophysical Research: Atmospheres*, *125*, e2019JD031730. https://doi.org/10.1029/2019JD031730

Wang, D., & Takagi, N. (2012a). Characteristics of winter lightning that occurred on a windmill and its lightning protection tower in Japan. *IEEJ Transactions on Power and Energy*, *132*(6), 568–572. https://doi.org/10.1541/icejpes132.568

Wang, D., & Takagi, N. (2012b). Three unusual upward positive lightning triggered by other nearby lightning discharge activity. Paper presented at the 22nd International Lightning Detection Conference, Broomfield, CO, USA, 2012.

Wang, D., Takagi, N., Watanabe, T., Sakurano, H., & Hashimoto, M. (2008). Observed characteristics of upward leaders that are initiated from a windmill and its lightning protection tower. *Geophysical Research Letters*, *35*, L02803. https://doi.org/10.1029/2007GL032136

Wang, D., Wu, T., & Takagi, N. (2018). Charge structure of winter thunderstorm in Japan: A review and an update. *IEEJ Transactions on Power and Energy*, *138*(5), 310–314. https://doi.org/10.1541/ieejpes.138.310

Warner, T. A. (2012). Observations of simultaneous upward lightning from multiple tall structures. *Atmospheric Research*, *117*, 45–54. https://doi.org/10.1016/j.atmosres.2011.07.004

Warner, T. A., Cummins, K. L., & Orville, R. E. (2012). Upward lightning observations from towers in Rapid City, South Dakota and comparison with National Lightning Detection Network data, 2004–2010. *Journal of Geophysical Research*, *117*(D19), D19109. https://doi.org/10.1029/2012JD018346

Warner, T. A., Lang, T. J., & Lyons, W. A. (2014). Synoptic scale outbreak of self-initiated upward lightning (SIUL) from tall structures during the central U.S. blizzard of 1–2 February 2011. *Journal of Geophysical Research: Atmospheres*, *119*(15), 9530–9548. https://doi.org/10.1002/2014JD021691

Watanabe, N., Nag, A., Diendorfer, G., Pichler, H., Schulz, W., Rakov, V. A., & Rassoul, H. K. (2019). Characteristics of currents in upward lightning flashes initiated from the Gaisberg Tower. *IEEE Transactions on Electromagnetic Compatibility*, *61*(3), 705–718. https://doi.org/10.1109/TEMC.2019.2916047

Wilkes, R. A., Uman, M. A., Pilkey, J. T., & Jordan, D. M. (2016). Luminosity in the initial breakdown stage of cloud -to-ground and intracloud lightning. *Journal of Geophysical Research: Atmospheres*, *121*(3), 1236–1247. https://doi.org/10.1002/2015JD024137

Williams, E. R. (2006). Problems in lightning physics—The role of polarity asymmetry. *Plasma Sources Science and Technology*, *15*(2), S91–S108. https://doi.org/10.1088/0963-0252/15/2/S12

Wu, B., Lyu, W., Qi, Q., Ma, Y., Chen, L., Zhang, Y., et al. (2019). Synchronized two-station optical and electric field observations of multiple upward lightning flashes triggered by a 310-kA +CG flash. *Journal of Geophysical Research: Atmospheres*, *124*(2), 1050–1063. https://doi.org/10.1029/2018JD029378

Wu, T., Wang, D., Rison, W., Thomas, R. J., Edens, H. E., Takagi, N., & Krehbiel, P. R. (2017). Corona discharges from a windmill and its lightning protection tower in winter thunderstorms. *Journal of Geophysical Research: Atmospheres*, *122*(9), 4849–4865. https://doi.org/10.1002/2016JD025832

Wu, T., Wang, D., & Takagi, N. (2018). Lightning mapping with an array of fast antennas. *Geophysical Research Letters*, *45*(8), 3698–3705. https://doi.org/10.1002/2018GL077628

Wu, T., Wang, D., & Takagi, N. (2019). Velocities of positive leaders in intracloud and negative cloud-to-ground lightning flashes. *Journal of Geophysical Research: Atmospheres*, *124*(17-18), 9983–9995. https://doi.org/10.1029/2019JD030783

Wu, T., Yoshida, S., Akiyama, Y., Stock, M., Ushio, T., & Kawasaki, Z. (2015). Preliminary breakdown of intracloud lightning: Initiation altitude, propagation speed, pulse train characteristics, and step length estimation. *Journal of Geophysical Research: Atmospheres*, *120*(18), 9071–9086. https://doi.org/10.1002/2015JD023546

Wu, T., Yoshida, S., Ushio, T., Kawasaki, Z., Takayanagi, Y., & Wang, D. (2014). Large bipolar lightning discharge events in winter thunderstorms in Japan. *Journal of Geophysical Research: Atmospheres*, *119*(2), 555–566. https://doi.org/10.1002/2013jd020369

Yoshida, S., Biagi, C. J., Rakov, V. A., Hill, J. D., Stapleton, M. V., Jordan, D. M., et al. (2010). Three-dimensional imaging of upward positive leaders in triggered lightning using VHF broadband digital interferometers. *Geophysical Research Letters*, *37*, L05805. https://doi.org/10.1029/2009GL042065

Yuan, S., Jiang, R., Qie, X., Wang, D., Sun, Z., & Liu, M. (2017). Characteristics of upward lightning on the Beijing 325 m meteorology tower and corresponding thunderstorm conditions. *Journal of Geophysical Research: Atmospheres*, *122*(22), 12,093–12,105. https://doi.org/10.1002/2017JD027198

Zheng, D., Shi, D., Zhang, Y., Zhang, Y., Lyu, W., & Meng, Q. (2019). Initial leader properties during the preliminary breakdown processes of lightning flashes and their associations with initiation positions. *Journal of Geophysical Research: Atmospheres*, *124*(14), 8025–8042. https://doi.org/10.1029/2019JD030300

Zheng, D., Wang, D., Zhang, Y., Wu, T., & Takagi, N. (2019). Charge regions indicated by LMA lightning flashes in Hokuriku's winter thunderstorms. *Journal of Geophysical Research: Atmospheres*, *124*, 7179–7206. https://doi.org/10.1029/2018JD030060

Zhou, H., Diendorfer, G., Thottappillil, R., Pichler, H., & Mair, M. (2012a). Characteristics of upward positive lightning flashes initiated from the Gaisberg Tower. *Journal of Geophysical Research*, *117*(D6), D06110. https://doi.org/10.1029/2011JD016903

Zhou, H., Diendorfer, G., Thottappillil, R., Pichler, H., & Mair, M. (2012b). Measured current and close electric field changes associated with the initiation of upward lightning from a tall tower. *Journal of Geophysical Research*, *117*(D8), D08102. https://doi.org/10.1029/2011JD017269

Zhu, Y., Ding, Z., Rakov, V. A., & Tran, M. D. (2019). Evolution of an upward negative lightning flash triggered by a distant +CG from a 257-m-tall tower, including initiation of subsequent strokes. *Geophysical Research Letters*, *46*. https://doi.org/10.1029/2019GL083274